J. Phys. G: Nucl. Part. Phys. 21 (1995) 1205–1216. Printed in the UK

Solution of the cranked harmonic oscillator model at non-zero temperatures

L Jacak†, W Nawrocka‡, R G Nazmitdinov§ and A Wójs†

† Institute of Physics, Technical University of Wrocław, Wybrzeże Wyspiańskiego 27, 50-370 Wrocław, Poland

‡ Institute of Theoretical Physics, University of Wrocław, Pl. M Borna 9, 50-205 Wrocław, Poland

§ Laboratory of Theoretical Physics, Joint Institute of Nuclear Research, Dubna, Head Post Office, PO Box 79, Moscow, Russia

Received 31 January 1995, in final form 27 June 1995

Abstract. The thermodynamics of the cranked anisotropic harmonic oscillator model of the nucleus is studied within the grand canonical ensemble. The equilibrium shape of the system is determined with respect to temperature and number of particles, both with and without rotation. A series of sharp deformation transitions, closely correlated with the harmonic-oscillator shell stucture, are found for the rotating system at sufficiently low temperatures.

1. Introduction

Let us consider the system of $\mathcal{N}$ nucleons in the rotating deformed harmonic oscillator potential as the grand canonical ensemble described by the temperature T and the chemical potential μ. The deformation of the system is described by the anisotropic oscillator frequencies ω_x, ω_y, ω_z (connected with the Hill–Wheeler ellipsoidal deformation parameters β and γ). These parameters are assumed to be functions of temperature, number of particles and total angular momentum of the system. As these parameters enter the Hamiltonian we deal with the effective theory with intrinsic anisotropy. The equilibrium shape of the system is found by minimization of the thermodynamical potential with respect to ω_x, ω_y, ω_z, ω and μ (deformation parameters, angular velocity of the whole system and chemical potential, respectively), provided that temperature, number of particles and total angular momentum are fixed.

The novelty of this approach relies on inclusion of the temperature-dependent thermodynamic mixture of all various quantum states instead of a sole, arbitrary chosen state, which was done previously in the investigations of the same model (e.g. works by Bohr and Mottelson [1], Kinouchi *et al* [4], Ripka *et al* [7], Stamp [10], Troudet and Arvieu [11], Zelevinski [12]). Let us underline that even though the thermalization procedure is rather widespread within nuclear theory (e.g. Goodman [2], Sato [9]), the analysis of even a simplified model, as presented in this paper, would be significant since it is exact and complete, and may be helpful in understanding the rotation of heated nuclei within a more realistic approach.

0954-3899/95/091205+12$19.50

2. Formalism

The effective cranked Hamiltonian considered has the form (in the rotating reference frame, rotation around the x-axis):

$$\hat{H}^{\omega} = \sum_{i=1}^{\mathcal{N}} (\hat{h}^{\omega})_i \tag{1}$$

where

$$\hat{h}^{\omega} = \hat{h}_0 - \hbar\omega\hat{l}_x \tag{2}$$

$$\hat{h}_0 = \frac{\hat{p}_x^2 + \hat{p}_y^2 + \hat{p}_z^2}{2m} + \frac{m}{2}(\omega_x^2 x^2 + \omega_y^2 y^2 + \omega_z^2 z^2) \tag{3}$$

ω is the cranking angular velocity, $\hat{l}_x$ is the x-component of the single-particle angular momentum. The eigenenergies of this Hamiltonian have the form:

$$\varepsilon_{\alpha}^{\omega} = \hbar\omega_x(n_x + \tfrac{1}{2}) + \hbar\omega_+(n_+ + \tfrac{1}{2}) + \hbar\omega_-(n_- + \tfrac{1}{2}) \tag{4}$$

where $\alpha = (n_x, n_+, n_-)$ and

$$\omega_{\pm}^2 = \frac{1}{2}(\omega_y^2 + \omega_z^2 + 2\omega^2) \pm \frac{1}{2}\sqrt{(\omega_y^2 - \omega_z^2)^2 + 8\omega^2(\omega_y^2 + \omega_z^2)}. \tag{5}$$

Within the thermodynamical approach with the inclusion of temperature, we have to average the dynamical variables over the grand canonical ensemble. This procedure, in contrast to the previous considerations, removes the restriction to the sole quantum configuration with fixed energy. Instead, we demand that temperature is a fixed parameter.

We use the grand canonical potential $\Omega = -k_B T \ln \mathcal{Z}$ (k_B is the Boltzmann constant) corresponding to the partition function $\mathcal{Z} = \mathrm{Tr}\exp[-(\hat{H}^{\omega} - \mu\hat{N})/k_B T]$. In this ensemble the occupation numbers of single-particle levels follow the Fermi distribution. In order to be able to manage with the fixed average number of particles $\mathcal{N}$ and fixed average total angular momentum $\mathcal{L}$ we now perform the Legendre transformation and introduce the following new potential:

$$\Phi = \Omega + \hbar\omega\langle\hat{L}_x\rangle + \mu\langle\hat{N}\rangle. \tag{6}$$

Here $\hat{L}_x = \sum_i (\hat{l}_x)_i$ and $\hat{N}$ is the operator of the number of particles, and we assume $\langle\hat{L}_x\rangle = \mathcal{L}$ and $\langle\hat{N}\rangle = \mathcal{N}$. This procedure leads to the substitution of the role of ω with $\mathcal{L}$, and of μ with $\mathcal{N}$. Therefore we deal with three fixed external parameters: T, $\mathcal{N}$, $\mathcal{L}$ (instead of T, μ, ω). The intrinsic variables are ω_x, ω_y, ω_z, ω and μ.

We assume additionally (after Stamp [10], Troudet and Arvieu [11]) the non-compressibility condition imposed on ω_x, ω_y and ω_z, which makes them mutually dependent. Having in mind a rich discussion of the form of this condition (Kinouchi *et al* [4], Ripka *et al* [7], Stamp [10]), we choose it as the conservation of potential volume

$$\omega_x\omega_y\omega_z = \omega_0^3 = \text{const.} \tag{7}$$

Parameter ω_0 can be in general a function of temperature, but even for temperature-independent ω_0 the average volume of the system $\langle V\rangle = \sqrt{\langle x^2\rangle\langle y^2\rangle\langle z^2\rangle}$ grows with increasing temperature as the nucleons spread to the higher single-particle orbitals (as demonstrated similarly by Sato [9]). One can introduce the thermal dependence of ω_0 via an additional condition imposed for example in the form: $\omega_0\langle V\rangle = \text{const}$. Nevertheless, within the considered model, ω_0 plays only the role of a scaling parameter at each temperature independently, and its conceivable dependence on temperature does not influence the results qualitatively, leading only to rescaling.

Assuming the system to be in equilibrium we write out the necessary conditions for the minimum of the potential Φ:

$$\frac{\partial\Phi}{\partial\omega_x}=0 \qquad \frac{\partial\Phi}{\partial\omega_y}=0 \qquad \frac{\partial\Phi}{\partial\omega_z}=0 \qquad \frac{\partial\Phi}{\partial\omega}=0 \qquad \frac{\partial\Phi}{\partial\mu}=0 \quad (8)$$

supplemented with equation (7). The above equations together with the definition (6) of the potential Φ lead to (from now on setting $\hbar$ and k_B to unity):

$$\omega_x^2\langle x^2\rangle=\omega_y^2\langle y^2\rangle \tag{9a}$$

$$=\omega_z^2\langle z^2\rangle \tag{9b}$$

$$\langle 1\rangle=\mathcal{N} \tag{9c}$$

$$m\omega(\langle y^2\rangle+\langle z^2\rangle)-\frac{4\omega}{\omega_+^2-\omega_-^2}(\langle n_+ +\tfrac{1}{2}\rangle\omega_+-\langle n_- +\tfrac{1}{2}\rangle\omega_-)=\mathcal{L} \tag{9d}$$

$$\omega_x\omega_y\omega_z=\omega_0^3 \tag{9e}$$

where the average spatial dimensions are

$$\langle x^2\rangle=\frac{1}{m}\frac{\langle n_x+\frac{1}{2}\rangle}{\omega_x} \tag{10a}$$

$$\langle y^2\rangle=\frac{1}{2m}\left[\frac{1+\mathcal{A}}{\omega_+}\langle n_+ +\tfrac{1}{2}\rangle+\frac{1-\mathcal{A}}{\omega_-}\langle n_- +\tfrac{1}{2}\rangle\right] \tag{10b}$$

$$\langle z^2\rangle=\frac{1}{2m}\left[\frac{1+\mathcal{B}}{\omega_+}\langle n_+ +\tfrac{1}{2}\rangle+\frac{1-\mathcal{B}}{\omega_-}\langle n_- +\tfrac{1}{2}\rangle\right] \tag{10c}$$

with $\mathcal{A}=(\omega_y^2-\omega_z^2+4\omega^2)/(\omega_+^2-\omega_-^2)$ and $\mathcal{B}=(\omega_z^2-\omega_y^2+4\omega^2)/(\omega_+^2-\omega_-^2)$. Statistical averaging has the form:

$$\langle\ldots\rangle=\mathrm{Tr}(\mathrm{e}^{-\beta\hat{H}}\ldots)=\sum_\alpha\{\exp[(\varepsilon_\alpha^\omega-\mu)/k_BT]+1\}^{-1}\ldots\ .$$

Equation (9*a*, *b*) is the condition for the minimum of the potential Ω with respect to the shape parameters, (9*c*) sets the average number of particles to $\mathcal{N}$, (9*d*) sets the average angular momentum to $\mathcal{L}$, and (9*e*) is the non-compressibility condition (7). Substituting formula (10) into the system (9) one can rewrite the latter in the following equivalent form:

$$\frac{1+\mathcal{A}}{\omega_+}\langle n_+ +\tfrac{1}{2}\rangle+\frac{1-\mathcal{A}}{\omega_-}\langle n_- +\tfrac{1}{2}\rangle=2\frac{\omega_x}{\omega_y^2}\langle n_x+\tfrac{1}{2}\rangle \tag{11a}$$

$$(\omega_y-\omega_z)\left(\frac{\omega_+^2+\omega^2}{\omega_+}\langle n_+ +\tfrac{1}{2}\rangle+\frac{\omega_-^2+\omega^2}{\omega_-}\langle n_- +\tfrac{1}{2}\rangle\right)=0 \tag{11b}$$

$$\langle 1\rangle=\mathcal{N} \tag{11c}$$

$$\frac{1+\mathcal{C}}{\omega_+}\langle n_+ +\tfrac{1}{2}\rangle+\frac{1-\mathcal{C}}{\omega_-}\langle n_- +\tfrac{1}{2}\rangle=-\frac{\mathcal{L}}{\omega} \tag{11d}$$

$$\omega_x\omega_y\omega_z=\omega_0^3 \tag{11e}$$

where $\mathcal{A}$ is defined as in equation (10) and $\mathcal{C}=2(\omega_y^2+\omega_z^2)/(\omega_+^2-\omega_-^2)$.

3. Results and discussion

Let us begin with the solution of the system (11) in the zero-angular-momentum limit. In this case the angular velocity ω in equilibrium is zero for any temperature and number of particles—no rotation in the laboratory frame. The dependences of the deformation and

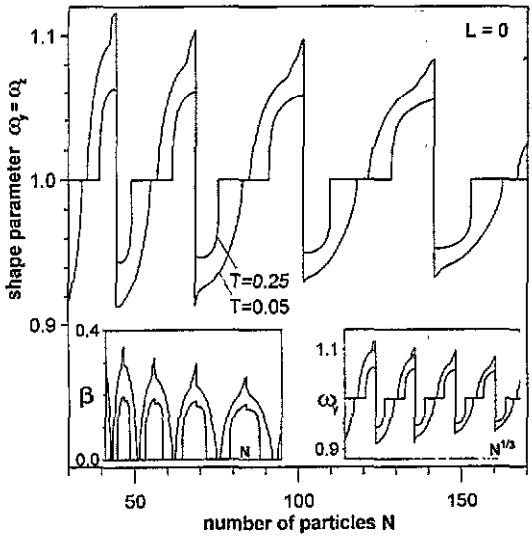

Figure 1. Spontaneous (without rotation) deformations of the many-fermion system confined to the anisotropic harmonic oscillator, with respect to the number of particles $\mathcal{N}$. Insets show equal quasi-periods in deformation plotted against the $\mathcal{N}^{1/3}$ coordinates (right-hand side) and the Hill–Wheeler deformation parameter β plotted against $\mathcal{N}$ (left-hand side).

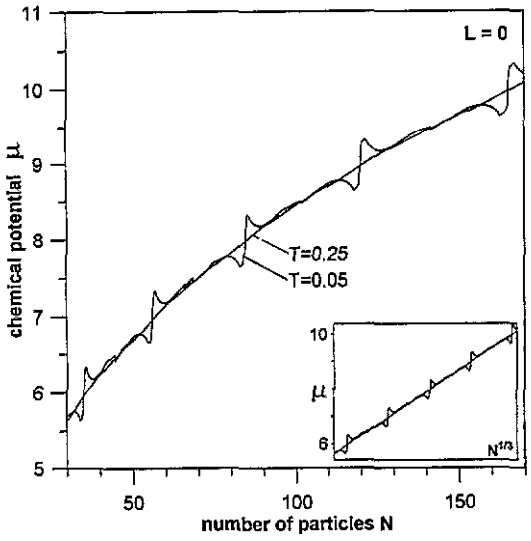

Figure 2. Dependence of the chemical potential μ on the number of particles $\mathcal{N}$, corresponding to figure 1. The inset shows equal quasi-periods in μ against $\mathcal{N}^{1/3}$ coordinates. Visible sharp jumps of the chemical potential near 'magic' numbers $\mathcal{N}$ indicate closed nuclear shells.

the chemical potential on the number of particles calculated for $T = 0.05$ and $T = 0.25$ (in ω_0 units) have been presented in figures 1 and 2. At low temperatures ($T < 0.3$ in ω_0 units) the equilibrium shape of the non-rotating system strongly depends on the number of particles, being spherical only in some intervals of $\mathcal{N}$. These intervals narrow with decreasing temperature and in the limit $T \to 0$ reduce to the 'magic' numbers, corresponding to the closed shells. The chemical potential undergoes sharp steps at the 'magic' numbers $\mathcal{N}$ which indeed indicate the stable configurations (the fluctuation of the number of particles given by $\langle\hat{N}^2\rangle - \langle\hat{N}\rangle^2 = k_B T\ \partial\mathcal{N}/\partial\mu$ appears to be close to zero). A direct consequence of the occurence of the shell structure is the quasi-periodic character of the deformation and μ as functions of $\mathcal{N}$. In the case of the harmonic-oscillator model the length of the quasi-period is constant against $\mathcal{N}^{1/3}$—see insets in figures 1 and 2. The harmonic-oscillator shell structure for zero temperature was originally described by Bohr and Mottelson [1]. It can be mentioned that although the number of particles in nuclei is

limited to the order of 100 which leads to only a few 'magic' numbers, a similar model is applicable to alkaline metal drops for which $\mathcal{N}$ can be much larger (cf work by Reimann *et al* [6], and references therein). Outside the 'magic' intervals the system is deformed to a biaxial ellipsoid, having rotational symmetry along a spontaneously chosen axis (the x-axis in figure 1). The deformations decay with the growth of temperature and for approximately $T > 0.3$ disappear completely—the system is spherical for all numbers of particles.

It is convenient to introduce the Hill–Wheeler parametrization (see, for example, Troudet and Arvieu [11]) for describing the deformation of an ellipsoid:

$$\sqrt{\langle x^2\rangle} = R_0 \cdot \exp\left[\sqrt{\frac{5}{4\pi}}\beta\cos\left(\gamma - \frac{4\pi}{3}\right)\right]$$

$$\sqrt{\langle y^2\rangle} = R_0 \cdot \exp\left[\sqrt{\frac{5}{4\pi}}\beta\cos\left(\gamma - \frac{2\pi}{3}\right)\right]$$

$$\sqrt{\langle z^2\rangle} = R_0 \cdot \exp\left[\sqrt{\frac{5}{4\pi}}\beta\cos\gamma\right]. \tag{12}$$

As the non-rotating nucleus is biaxial, we have $\gamma = \pi/3$ *for* $\omega_y < 1$ *(oblate symmetry) and* $\gamma = 0$ for $\omega_y > 1$ (prolate symmetry). The dependence of β on $\mathcal{N}$ has been shown in the inset in figure 1.

Since the low-temperature shell structure is specific for the anisotropic oscillator model, we deal in general with two qualitatively distinct cases of the non-rotating system: deformed or spherical. Hence, the analysis of the rotation will be illustrated with the computations performed for $\mathcal{N} = 100$ and $\mathcal{N} = 120$, corresponding to the strong deformation and the spherical shape without rotation, respectively.

Now we pass on to solving (11) for non-zero $\mathcal{L}$. One can recognize that we deal with a system of highly nonlinear equations with multivalued solutions. Due to the form of equation (11*b*) the solutions of the whole system split into two types: axially symmetrical, with $\omega_y = \omega_z$—corresponding to the biaxial ellipsoid with the angular momentum along the axis of symmetry, and non-axial, with $\omega_y \neq \omega_z$—corresponding to the triaxial ellipsoid rotating around one of the principal axes. The former case needs some clarification as the transformation to the rotating reference frame is non-unique from a quantum point of view and hence cannot be performed. Consequently, the nucleus cannot undergo collective rotation in this regime. The state in which the system has non-zero total angular momentum and axial symmetry is however possible as the result of non-collective motions of the individual nucleons on axially symmetrical orbitals (cf Bohr and Mottelson [1], Goodman [3], Nawrocka *et al* [5]). In this case $\mathcal{L}$ is a sum of the single-body angular momenta l_x, which are good quantum numbers here. It can be admitted that despite the axial symmetry, the nuclei of different $\mathcal{L}$ are distinguishable due to the axial deformation resulting from the occupation by some of the nucleons of the states with higher l_x (above the Fermi level). Despite the distinct physical background, we proceed formally and arrive at the axial case of the system of equations (11) obtained from the cranking procedure (2). The quantity ω however cannot be interpreted as angular velocity for non-collective motion and is only a parameter in the Legendre transformation. In this case ($\omega_y = \omega_z$) we have $\omega_\pm = \omega_y \pm \omega$ and the system (11) reduces to

$$\omega_y\langle n_+ + n_- + 1\rangle = \omega_x\langle 2n_x + 1\rangle \tag{13a}$$

$$\omega_y = \omega_z \tag{13b}$$

$$\langle 1\rangle = N \tag{13c}$$

$$\langle n_- - n_+ \rangle = \mathcal{L} \tag{13d}$$

$$\omega_x \omega_y \omega_z = \omega_0^3. \tag{13e}$$

Let us now examine in more detail the non-axial solutions of the system (11). By direct calculation one can find out that for low temperatures there exists a very rich family of solutions of the system (13) following the irregular behaviour of potential Φ (with a great number of extrema) as a function of the shape of nucleus. The solution of physical importance (thermodynamically stable) is the one at which the thermodynamical potential Φ reaches the global minimum (it is the minimal envelope of the collection of all solutions of (11)). This solution is the piece-wise continuous function of $\mathcal{L}$. The discontinuous changes of variables ω_x, ω_y and ω_z determine the phase transitions of the deformation of a nucleus.

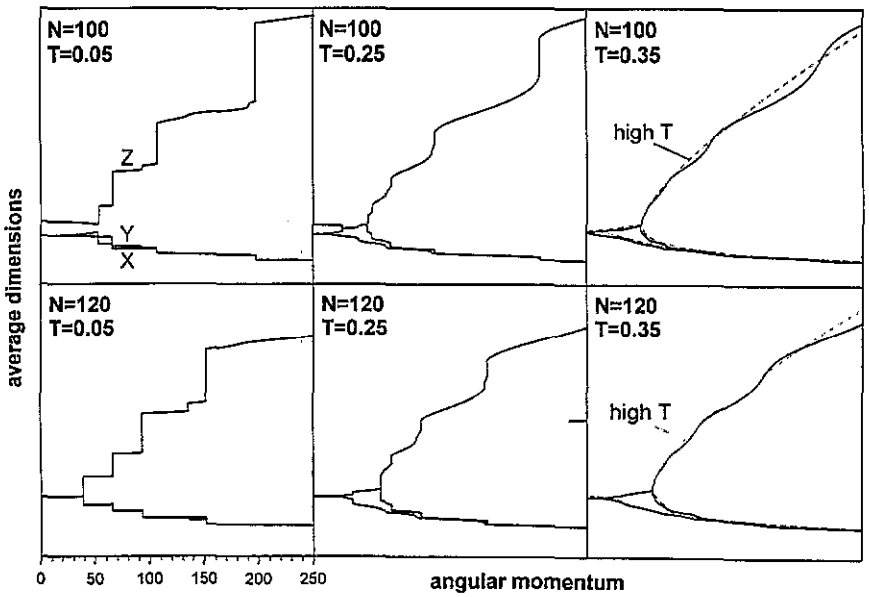

Figure 3. Dependence of the average spatial dimensions of the system (ellipsoid semi-axes X, Y and Z) on the angular momentum $\mathcal{L}$, for particle numbers $\mathcal{N} = 100$, 120, and temperatures $T = 0.05$, 0.25, 0.35. Both horizontal and vertical axes are common for all frames. The thin dashed lines in frames for $T = 0.35$ correspond to $T = 1$.

In figures 3–7 the stable solutions of the system (11) have been presented both for $\mathcal{N} = 100$ and 120 and $T = 0.05$, 0.25, 0.35, 1.00 (all in units of ω_0 with $\hbar$ and k_B set to unity). In figure 3 the evolution of the average dimensions (ellipsoid semi-axes): $X = \sqrt{\langle x^2 \rangle}$, $Y = \sqrt{\langle y^2 \rangle}$ and $Z = \sqrt{\langle z^2 \rangle}$, in increasing $\mathcal{L}$ has been plotted, figure 4 presents corresponding trajectories in the Hill–Wheeler (β, γ) plane, while in figures 5–7 we present corresponding graphs for μ, ω and Φ against $\mathcal{L}$.

For both systems, $\mathcal{N} = 100$ and 120, corresponding to the deformed and spherical non-rotating shapes respectively, we observe the continuous transition from low-temperature behaviour with numerous step-like changes in the deformation accompanied by discontinuities in the chemical potential, angular velocity, moment of inertia etc, to the characteristic classical picture with a single phase transition separating regions of oblate symmetry (MacLaurin sequence) and triaxial shape tending to the prolate symmetry in the high $\mathcal{L}$ limit (Jacobi sequence). A common property of the behaviour of the angular velocity ω with respect to $\mathcal{L}$ (for both nuclei and at both low and high temperatures) is the occurrence

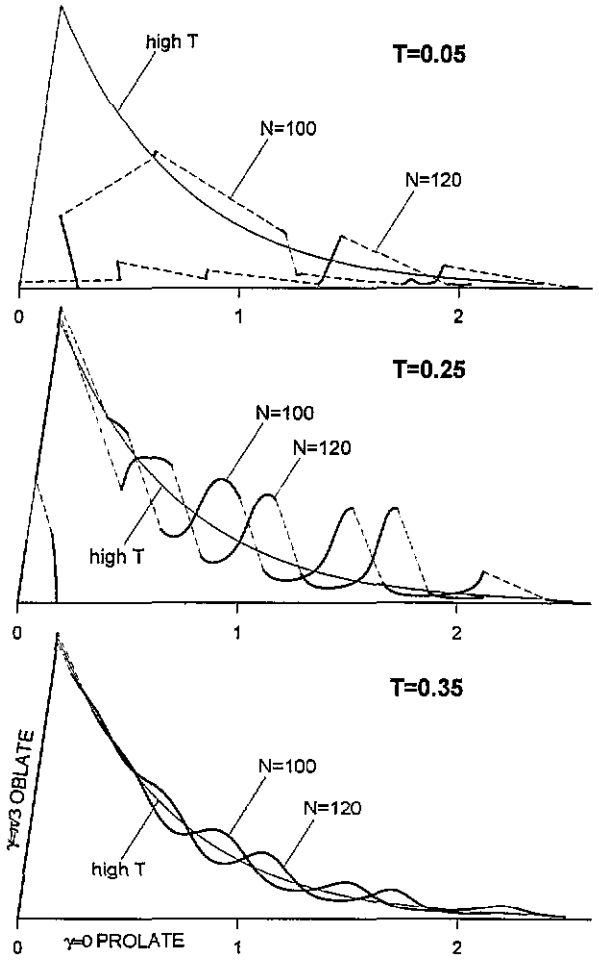

Figure 4. Evolution of the shape with increasing angular momentum, corresponding to figure 3, shown as trajectories in the Hill–Wheeler (β, γ) plane. High-T curves have been obtained for $T = 1$. For clarity the plane has been stretched vertically (×3).

of the maximum very close to the high-temperature Jacobi point. Since scaling energy ω_0 is the distance between single-particle energy levels for a non-rotating spherical nucleus, and T is of the order of the thermal spread, it is expected that at $T = 1$ (in ω_0 units) all quantum effects disappear and classical behaviour is realized.

For $\mathcal{N} = 100$ at very low temperatures (the curves for $T = 0.05$ in figures 3–7) a nucleus begins rotation (small $\mathcal{L}$) around the axis perpendicular to the axis of symmetry (prolate shape) and continues motion for higher values of $\mathcal{L}$ with the shape very close to prolate with a bigger deviation only in the region of $\mathcal{L} = 50$. For a little higher temperature a narrow region appears below $\mathcal{L} = 50$ where an oblate shape is favourable. This region expands with the growth of temperature, being $\mathcal{L} = 27$–50 for $T = 0.25$, and reaching the whole range $\mathcal{L} = 0$–50 close to $T = 0.35$. Simultaneously, all discontinuities except the axial–non-axial transition gradually disappear. Further increase in T only flattens the signs of the low-temperature steps and around $T = 1$ the curves practically reach the limiting high-T shapes.

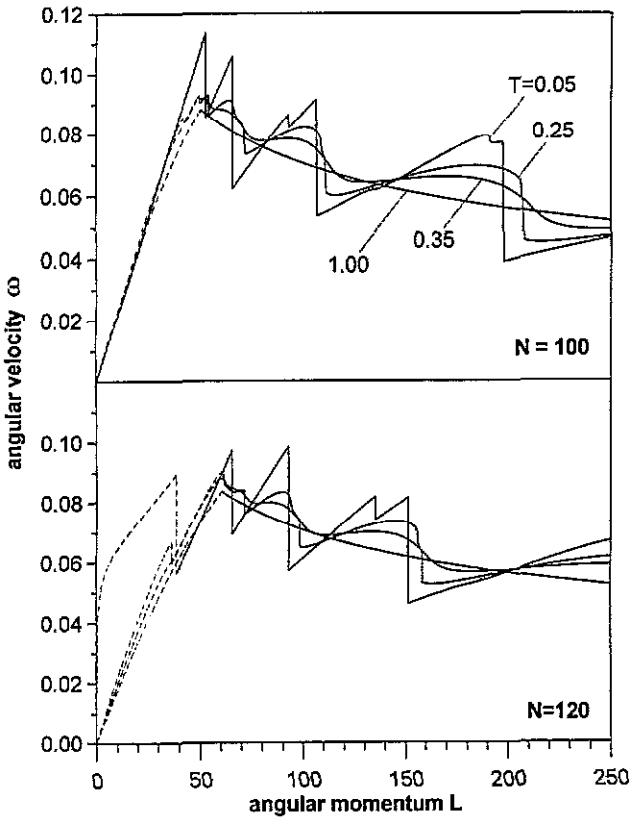

Figure 5. Dependences of the angular velocity ω on the angular momentum $\mathcal{L}$, corresponding to the curves in figure 3. Dashed lines indicate the axial-symmetry solutions, which do not describe collective rotation.

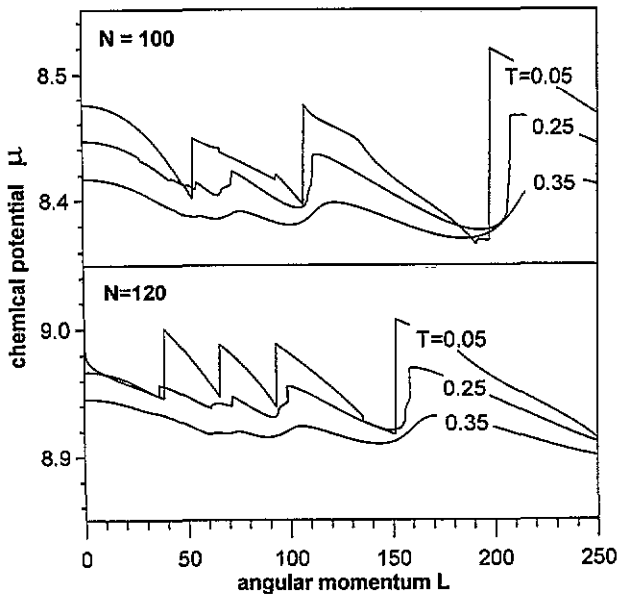

Figure 6. Dependences of the chemical potential μ on the angular momentum $\mathcal{L}$, corresponding to the curves in figure 3.

For $\mathcal{N} = 120$, in contrast to the previous case, even at very low temperatures the rotation begins in the oblate regime and motion continues around the axis of symmetry up to a critical value of $\mathcal{L}$ (38.5 for $T = 0.05$) from where the equilibrium shape is close to

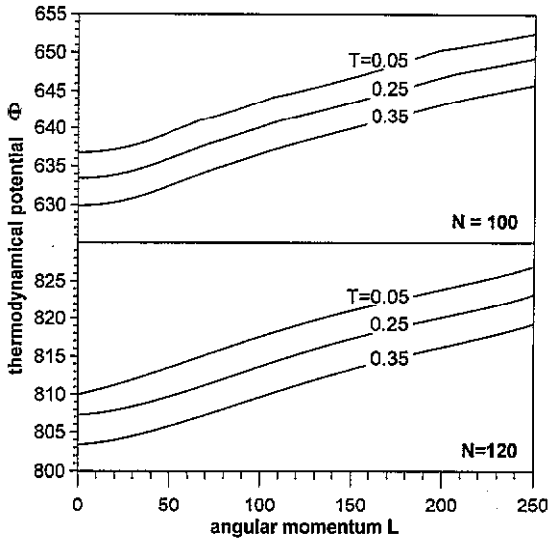

Figure 7. Dependences of the thermodynamical potential Φ on the angular momentum $\mathcal{L}$, corresponding to the curves in figure 3.

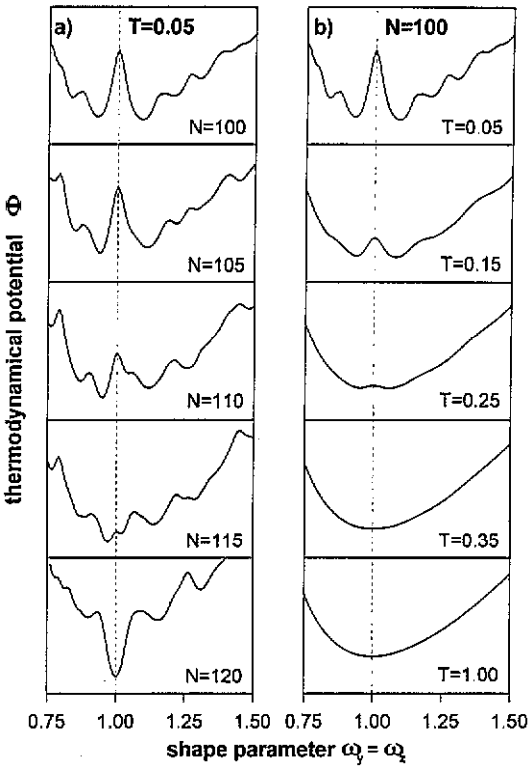

Figure 8. Typical dependences of the thermodynamical potential Φ on the deformation. Two-dimensional graphs are obtained as sections of three-dimensional surface $\Phi(\omega_y, \omega_z)$ along direction $\omega_y = \omega_z$. (a) Fixed temperature $T = 0.05$ and varied number of particles $\mathcal{N}$, (b) fixed number of particles $\mathcal{N} = 100$ and varied temperature T.

prolate. Similarly as in the case of $\mathcal{N} = 100$ the growth of temperature gradually smooths the curves and broadens the oblate regime region, which is $\mathcal{L} = 0$–61 at $T = 1$. The high-temperature behaviour of both nuclei is qualitatively the same, as the effect of the filled shell does not appear in that case.

It is also interesting to observe that the potential Φ for the equlibrium state is always a continuous, regular function despite the sharp step-type deformation transitions at low

temperatures (see figure 7). Typical graphs of this potential as a function of the shape parameter for a non-rotating system are shown in figure 8—for a few values of $\mathcal{N}$ at fixed $T = 0.05$ in (8*a*), and for a few values of T at fixed $\mathcal{N} = 100$ in (8*b*). The graphs have been obtained as the sections of three-dimensional surface $\Phi(\omega_y, \omega_z)$ along the direction $\omega_y = \omega_z$. Since we know that for $\mathcal{L} = 0$ the equilibrium shape is always axially symmetrical, this section is sufficient to observe how the equilibrium shape is chosen as a result of the competition between different minima of Φ. Thus, in (8*a*) we can see how the discontinuous change of the shape as a function of the number of particles takes place around $\mathcal{N} = 100$, and how filling of the shell is reflected in the dependence of Φ on the deformation. In (8*b*) it is easy to observe the effect of thermal spreading.

An additional important result is that for the stable (minimum of Φ) solutions of equations (11) the collective rotation is, with good accuracy, a rigid-body rotation (with uniform density of mass), independent of temperature, number of nucleons and angular momentum. The deviation from the rigid-body regime appears as a second term in equation (9*d*), which for Φ-minimum solutions is very small compared to $\mathcal{L}$. Hence, we have $\mathcal{L} \approx m\omega(\langle y^2\rangle + \langle z^2\rangle)$. In figure 9 we have plotted the moment of inertia I_{rb}, calculated for a rigid body with the uniform distribution of mass: $I_{rb} = m(\langle y^2\rangle + \langle z^2\rangle)$, as a function of $\mathcal{L}$, for $\mathcal{N} = 100$ and 120, both for low and high temperatures ($T = 0.05$ and 1.00). The rigid-body angular momentum $\mathcal{L}_{rb} = \omega I_{rb}$ as a function of $\mathcal{L}$ is a straight line: $\mathcal{L}_{rb} = \mathcal{L}$. Let us underline that for other solutions of equations (11) (which do not minimize Φ) this is not true.

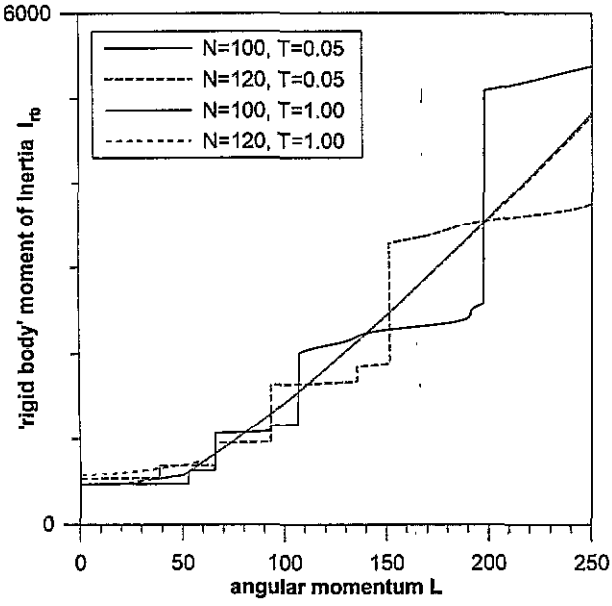

Figure 9. Moment of inertia calculated for the rigid-body rotation I_{rb} (in $\hbar/\omega_0$ units), as a function of the angular momentum $\mathcal{L}$. Numbers of particles $\mathcal{N} = 100$, 120. Temperatures $T = 0.05$, 1.00 (the $T = 1.00$ curves appear almost coincident in this figure).

It is also interesting to consider the high-temperature limit ($k_B T \geqslant \hbar\omega_0$) of the behaviour of a nucleus within this model (see also appendix). There are only two solutions of equations (11) in this case. One solution has axial symmetry and exists for all values of $\mathcal{L}$. It undergoes *an instability at a certain value* $\mathcal{L}_M$, *leading to the occurrence of a smooth maximum in* the dependence $\omega(\mathcal{L})$. This is called the MacLaurin sequence. However, above the critical value $\mathcal{L}_c < \mathcal{L}_M$ (bifurcation point) the triaxial solution appears and it tends to the prolate symmetry for high $\mathcal{L}$, which is energetically more favourable. Angular velocity ω decreases with increase of $\mathcal{L}$ in this solution. The change of the shape (and consequently also of the

other parameters such as ω, μ etc) in $\mathcal{L}_c$ is continuous and the corresponding phase transition is of second order. The instability in the bifurcation point $\mathcal{L}_c$ is called the Jacobi instability, and the whole triaxial solution the Jacobi sequence. The limiting high-T behaviour of the parameters ω, ω_{xyz}, $\mathcal{L}$ and μ in the transition point can be found:

$$\frac{\mathcal{L}_c}{\mathcal{N}} = \frac{1}{\sqrt{3}} - \frac{1}{12\sqrt{3}\sqrt[3]{2}}\left(\frac{\hbar\omega_0}{k_BT}\right)^2 + \dots \tag{14}$$

$$\frac{\omega_c}{\omega_0} = \frac{1}{2\sqrt{3}\sqrt[3]{2}}\cdot\frac{\hbar\omega_0}{k_BT} - \frac{5}{144\sqrt{3}\sqrt[3]{4}}\left(\frac{\hbar\omega_0}{k_BT}\right)^3 + \dots \tag{15}$$

$$\frac{\omega_0}{\omega_{xc}} = \left(\frac{\omega_{yc}}{\omega_0}\right)^2 = \left(\frac{\omega_{zc}}{\omega_0}\right)^2 = \frac{1}{\sqrt[3]{2}} + \frac{\sqrt[3]{2}}{144}\left(\frac{\hbar\omega_0}{k_BT}\right)^2 + \dots \tag{16}$$

$$\frac{\mu_c}{\hbar\omega_0} = \frac{k_BT}{\hbar\omega_0}\left(\ln\mathcal{N} + 3\ln\frac{\hbar\omega_0}{k_BT}\right) - \frac{1}{12\sqrt[3]{2}}\left(\frac{\hbar\omega_0}{k_BT}\right) + \dots . \tag{17}$$

Hence, in the high-T limit, the axial–non-axial transition takes place at the critical value of the average angular momentum per particle $(1/\sqrt{3})$. The deformation at the critical point tends to $\omega_{xc}/\omega_{yc} \to \sqrt{2}$, while the angular velocity ω_c, being at the same time the maximum angular velocity of the system in equilibrium, decays to zero with the growth of T. As was necessary for the classical-limit approximation we also get $\exp(\mu_c/k_BT) \to 0$. The dependences of the critical parameters on temperature, following equations (14)–(17), are shown in figure 10.

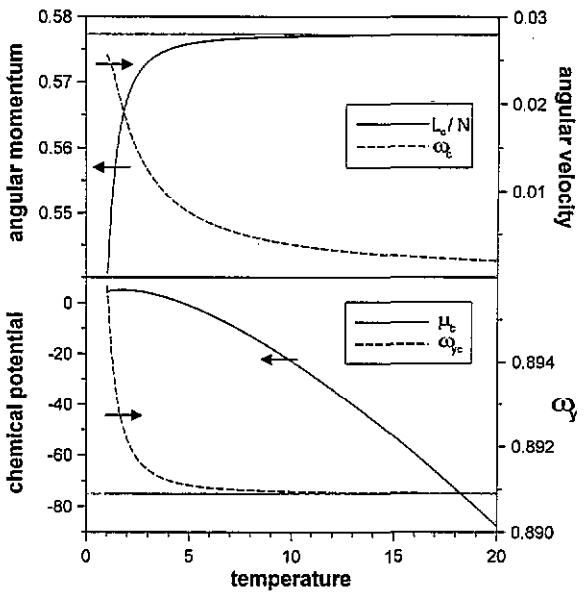

Figure 10. Thermal dependences of critical parameters at the high-temperature Jacobi transition; upper frame: angular momentum per single particle $\mathcal{L}_c/\mathcal{N}$ and angular velocity ω_c; lower frame: deformation parameter ω_{yc} and chemical potential μ_c. Straight horizontal lines correspond to the high-temperature limits of $\mathcal{L}_c/\mathcal{N}$ and ω_{yc} in the upper and lower frame, respectively.

In conclusion, let us summarize that for the equilibrium state of a nucleus within the cranked anisotropic harmonic oscillator model, at sufficiently low temperatures ($T < 0.3\omega_0$) we deal with the multiple first-order phase transitions of the shape. At high temperatures the evolution of the shape of a nucleus follows the MacLaurin and Jacobi sequences with a

single second-order phase transition. Despite the complicated behaviour of the shape, in the case of collective rotation, stable configurations for all $\mathcal{N}$, T and $\mathcal{L}$ correspond, with good accuracy, to the rigid-body regime. The phase transitions at low temperature originate from exchange interaction of fermions, which was taken into account by the minimizing procedure applied to the potential Φ. Let us also mention that the sharp deformation transitions at low temperatures would be smoothed by including the fluctuations, similarly demonstrated by Rossignoli *et al* [8].

Acknowledgments

This work has been supported by KBN Project No 2P 302 018 04

Appendix

In the high-temperature limit ($\exp[\mu/k_BT] \ll 1$) the summations in equations (11) can be performed analytically:

$$\langle 1\rangle = e^{\mu/k_BT}\left(8\sinh\frac{\hbar\omega_x}{2k_BT}\sinh\frac{\hbar\omega_+}{2k_BT}\sinh\frac{\hbar\omega_-}{2k_BT}\right)^{-1} \tag{18a}$$

$$\langle n_\zeta + 1/2\rangle = \langle 1\rangle\frac{1}{2}\coth\frac{\hbar\omega_\zeta}{2k_BT} \qquad \zeta = +, -, x. \tag{18b}$$

The thermodynamical potentials Ω and Φ are

$$\Omega = -k_BT\mathcal{N} \qquad \Phi = (\mu - k_BT)\mathcal{N} + \hbar\omega\mathcal{L} \tag{19}$$

with chemical potential:

$$\mu = k_BT\ln\left(8\mathcal{N}\sinh\frac{\hbar\omega_x}{2k_BT}\sinh\frac{\hbar\omega_+}{2k_BT}\sinh\frac{\hbar\omega_-}{2k_BT}\right). \tag{20}$$

Due to the continuous character of the transition in $\mathcal{L}_c$, we can calculate the critical parameters $\mathcal{L}_c$, ω_{xc}, ω_{yc}, ω_{zc}, ω_c and μ_c by solving the high-T version of the system (11) in the non-axial regime (the right-hand factor in (11*b*) must vanish) and then take the limit $\omega_y - \omega_z \to 0$. Thus, expanding $\coth x \approx 1/x + x/3$ (1.5% error for $x = 1$), formulae (14)–(17) are obtained.

References

[1] Bohr A and Mottelson B R 1974 *Nuclear Structure II* (Benjamin: New York)
[2] Goodman A L 1993 *Phys. Rev.* C **48** 2679
[3] Goodman A L 1994 *Phys. Rev. Lett.* **73** 416
[4] Kinouchi S, Kishimoto T, Kubo T, Sakamoto H and Kammuri T 1993 *Prog. Theor. Phys.* **89** 1203
[5] Nawrocka W, Nazmitdinov R G and Jacak L 1990 *Phys. Lett.* **238B** 131
[6] Reimann S M, Brack M and Hansen K 1993 *Z. Phys.* D **28** 235
[7] Ripka G, Blaizot J P and Kassis N 1975 *Heavy Ions High Spin States and Nuclear Structure* vol 1 (IAEA: Vienna) p 445
[8] Rossignoli R, Canosa N and Ring P 1994 *Phys. Rev. Lett.* **72** 4070
[9] Sato H 1987 *Phys. Rev.* C **36** 785
[10] Stamp A P 1978 *Z. Phys.* A **284** 305
[11] Troudet T and Arvieu R 1981 *Ann. Phys., NY* **134** 1
[12] Zelevinsky V G 1975 *Sov. J. Nucl. Phys.* **22** 565